

Extreme April heat in Spain, Portugal, Morocco & Algeria almost impossible without climate change

Sjoukje Philip¹, Sarah Kew¹, Robert Vautard², Izidine Pinto¹, Maja Vahlberg³, Roop Singh³, Fatima Driouech⁴, Redouane Lguensat², Clair Barnes⁵, Friederike Otto⁵

¹ *Royal Netherlands Meteorological Institute (KNMI), De Bilt, The Netherlands*

² *Institut Pierre-Simon Laplace, CNRS, Sorbonne Université, Paris, France*

³ *Red Cross Red Crescent Climate Centre, The Hague, the Netherlands*

⁴ *University Mohammed VI Polytechnic, Morocco*

⁵ *Grantham Institute, Imperial College London, UK*

Main findings

- Heatwaves are amongst the deadliest natural hazards with thousands of people dying from heat-related causes each year. However, the full impact of a heatwave is often not known until weeks or months afterwards, once death certificates are collected, or scientists can analyse excess deaths. Many places lack good record keeping of heat-related deaths, therefore currently available global mortality figures are likely an underestimate.
- Early heatwaves and associated drought conditions also threaten the yield for many crops such as wheat, because it hinders grain filling. This heatwave has come at a critical time for the crop season in the Western Mediterranean countries.
- While Europe and North Africa have experienced heatwaves increasingly frequently over the last years, the recent heat in the Western Mediterranean has been so extreme that it is also a rare event in today's warmer climate. Our estimate of observed temperatures averaged over 3 days were estimated to have a return period of approximately 400 years (at least 60 years) in the current climate, meaning they have approximately a 0.25% chance of happening in any given year.
- To estimate the influence of human-caused climate change on this extreme heat we combine climate models with the observations. Observations and models both show a strong increase in likelihood and intensity but the change is systematically lower in the models than in the observations. The fact that extreme heat is increasing faster than climate models simulate is a known problem in summer in Western Europe, in all climate models, and is also found here.
- The combined results, giving an increase in the likelihood of such an event to occur of at least a factor of 100, is therefore likely too conservative. At the same time, a heatwave with a chance of occurrence of 0.25% in any given year (return period of 1-in-400 years) would have been at least 2C cooler in a 1.2°C colder world.
- This discrepancies between the modelled and observed trends and variability also hinders confidence in projections of the future trends. In a future 0.8°C warmer climate (reaching a global warming of 2C above pre-industrial levels) such a heatwave would be another 1°C hotter, but as above, this is probably a very conservative estimate.
- Heat-related fatalities have decreased in cities with urban planning for extreme heat. This has proved effective in Spain, and notably in Lisbon, Portugal, where the urban heat island effect

has been reduced through incorporating more green and blue spaces. In addition, early warning systems for heat, simple self-protective behaviours such as drinking enough water, city heat action plans, strong social ties, and improved risk perception have been shown to reduce heat-related health impacts.

1 Introduction

Approaching the end of April 2023, countries bordering the western Mediterranean experienced an exceptional early heatwave, with local temperatures up to 20 degrees hotter than normal and April records being broken by up to 6 degrees. The national record for April was broken in Portugal, and in Mainland Spain, with respectively 36.9°C and 38.8°C measured in the Southernmost parts of the countries. In Morocco, several (local) April records have been broken across the country and temperatures exceeded 41°C in some cities such as Sidi-Slimane, Marrakech, Taroudant (Source: DGM, Morocco). Temperatures exceeded 40°C in Algeria on 28 April (Maghnia, Mascara-Ghriss at least).

The early season extreme heat has notably preponed the enforcement of the regional Action Plan for Episodes of High Temperatures (Plan de Actuación ante Episodios de Altas Temperaturas) for the Municipality of Madrid by a full month ([Comunidad de Madrid, 2023](#)). Along with the roll-out of an awareness raising campaign about the need to conserve water, hospitals began to monitor the admissions of patients with heat-related illnesses and health services' access to air conditioning, and educational institutions adjusted school and sports practice hours to avoid the hottest hours of the day ([La Opinión, 2023](#)). To further mitigate heat risk, floor cooling measures will be installed in public preschools, public pools will open one month earlier than usual, and public transportation will increase in frequency to avoid crowding and waiting ([Reuters, 2023](#); [La Opinión, 2023](#)). In Seville, one of the hottest parts of Spain, healthcare staffing and the budget for emergency services have both been significantly boosted ([Reuters, 2023](#)). On 28 April, the second day of Morocco Desert Challenge, a Dutch competitor reportedly passed away after suffering from heat stroke and exhaustion ([The Checkered Flag, 2023](#)).

The record shattering temperatures came on top of a historical multi-year drought in those regions. Drought is known to amplify extreme temperatures, when hydric stress in plants takes place and evapotranspiration is replaced by sensible heat fluxes ([Seneviratne et al., 2010](#)), under the conditions of specific weather regimes ([Quesada et al., 2012](#)). The high temperatures are also affecting the current drought, especially through the impact on agriculture. Water reservoirs in Spain are already up to 50% below average levels ([Sky News, 2023a](#); [The Local, 2023](#); [News24, 2023](#)) resulting in water restrictions ([The Local, 2023](#)) and over 80'000 people in Catalonia relying on trucks providing drinking water ([Sky News, 2023b](#); [CNN, 2023](#)). In Morocco, although some reservoirs are relatively well filled, the average dam storage was about 33% at the end of April ([Ministère de l'équipement et de l'eau, 2023](#)), which demonstrates the harmful effect of the consecutive dry years registered since 2020. In Tunisia, many homes no longer have running tap water for more than a few hours a day due to water restrictions, as water levels in some dams have decreased by 60-80% while others are completely dry, a record low ([Africa News, 2023](#), [People's Dispatch, 2023](#)). Across Spain and Tunisia alike, roughly 60% of farmland has been affected by drought, while Moroccan farmers anticipate another poor agricultural season on top of last year's, when Morocco experienced its most severe drought in 70 years ([The Local, 2023](#); [Asharq al-Awsat, 2023](#); [Atalayar, 2023](#)). Notably, Spain is experiencing what is on track to become the driest April on record, with below-average levels of rainfall over the past at least 36 months ([Earth Org, 2023](#); [The Local, 2023](#); [News24, 2023](#)). Beyond drought, this outstanding heat wave was

fostered by high radiation, anticyclonic clear-sky stagnant conditions with air masses in part from hot Saharan regions.

To define the event we use the April maximum of 3-day running mean daily maximum temperature (AprTX3x) averaged over land within 10°W to 5°E; 30°N to 40°N (Figure 1). This covers part of Portugal, Spain, Algeria and Morocco. Anomalies with respect to 1991-2020 are shown in Figure 1 for 26-28 April 2023.

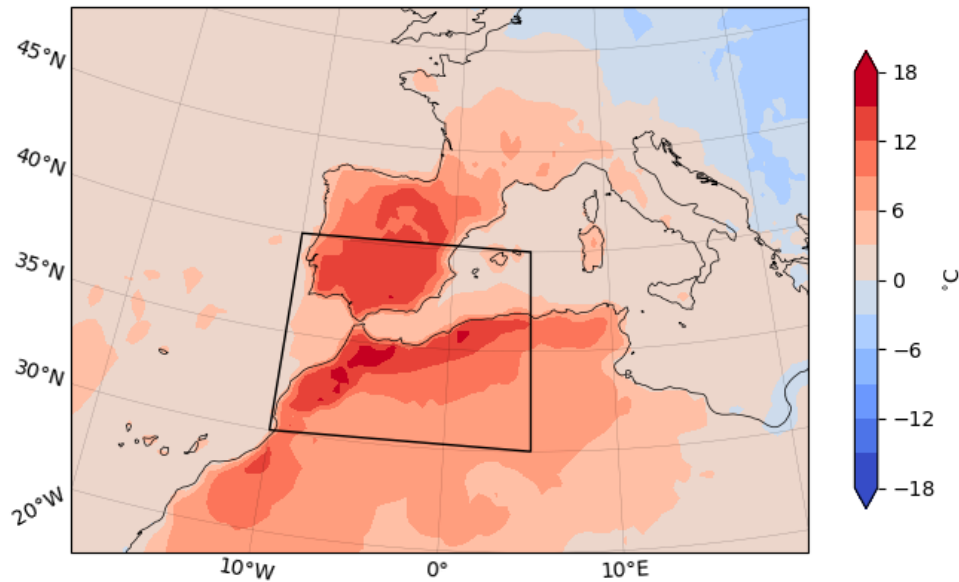


Figure 1. ERA5-extended maximum daily temperature anomalies with respect to 1991-2020 averaged over 26-28 April 2023. The black box outlines the study area.

This document is a short report on the heatwave, with more limited analysis as compared to regular World Weather Attribution studies. The analysis and the report are shorter, with less details; for the sake of rapidity, the analysis on impacts, vulnerability and exposure is shorter, the event definition uses a more standard index over a box area and is less tailored to impacts, no local dataset has been used and one multi-model ensemble is used. Standard methods are used as in regular studies. Furthermore, preliminary observational data have been used. This may have an influence on the estimated return period and observational results, although the influence on the overall result is assumed to be small. For more details on differences in the methods see Section 2.3.

The AR6 WGI report stresses that Mediterranean regions have in general already undergone increases in heat waves and agro-ecological droughts, attributable to climate change with respectively high and medium confidence ([Summary for Policy Makers](#), Figure 3), and that further climate change will induce many climatic impact drivers to increase with high confidence (see e.g. [Figure 12.11 CH12](#)) of the WGI AR6 assessment report. The current heatwave, together with the associated extreme drought, are therefore among the many consequences expected from climate change in this region.

2 Data and methods

2.1 Observational data

We use the European Centre for Medium-range Weather Forecasts (ECMWF) Re-Analysis product, ERA5, beginning in the year 1950 ([Hersbach et al., 2020](#)). We use maximum daily temperature (TX) from this product at $0.5^\circ \times 0.5^\circ$ horizontal resolution. It should be noted that the variables from ERA5 are not directly assimilated, but these are generated by atmospheric components of the Integrated Forecast System (IFS) modelling system. The re-analysis is available until the end of the preceding month (March 2023, at the start of the super-rapid study). We extend the re-analysis data with the ECMWF analysis (1-27 April) and the ECMWF forecast (28-30 April) to cover the period of the highest temperatures in April.

We use the global mean surface temperature (GMST) from the National Aeronautics and Space Administration (NASA) Goddard Institute for Space Science (GISS) surface temperature analysis (GISTEMP, [Hansen et al., 2010](#) and [Lenssen et al. 2019](#)) as an indicator of observed anthropogenic climate change. A smoothed four-year low-pass filter is applied to the GMST.

2.2 Model and experiment descriptions

In this super-rapid analysis, we use just one multi-model ensemble, CMIP6, in contrast to a full analysis where more than one climate modelling experiment would be considered from different framings ([Philip et al., 2020](#)). However, given the fact that all models underestimate the observed increase in heat extremes in Europe ([van Oldenborgh et al., 2022](#)) adding more models would in this case not have added much value, unless they were systematically different in the processes included. Such models are currently not available. Thus, while more models would lead to quantitatively different conclusions, qualitatively including any number of models leads to an overall lower increase in likelihood and intensity than observed.

At the time of analysis, we used 19 models with different horizontal resolutions from the ocean-atmosphere coupled global circulation model simulations that make up the CMIP6 multi-model ensemble. For details on CMIP6, please see [Eyring et al., \(2016\)](#). For all simulations, the period 1850 to 2015 is based on historical simulations, while the SSP5-8.5 scenario is used for the remainder of the 21st century. Each CMIP6 model has its own land-sea mask and this is used to select land-only grid cells in the study area for this analysis, keeping the native resolution of each model. Only one ensemble member from each model is analysed for AprTX3x. Each model's GMST is used as co-variate, smoothed with a 4-year running mean.

2.3 Statistical methods

We analyse time series of the April maximum of 3-day running mean daily maximum temperatures, AprTX3x averaged over land within the west Mediterranean study box, 10°W to 5°E ; 30°N to 40°N (Fig 1). Methods for observational and model analysis and for model evaluation and synthesis are generally used according to the World Weather Attribution Protocol, described in [Philip et al. \(2020\)](#), with supporting details found in van [Oldenborgh et al. \(2021\)](#), [Ciavarella et al. \(2021\)](#) and [World Weather Attribution \(WWA\)](#).

The analysis steps include: (i) trend calculation from observations or reanalyses; (ii) model evaluation; (iii) multi-method multi-model attribution and (iv) synthesis of the attribution statement.

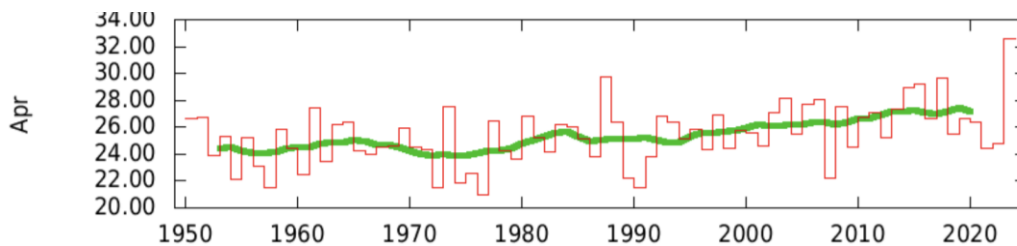
We calculate the return periods, Probability Ratio (PR; the factor-change in the event's probability) and change in intensity of the event under study in order to compare the climate of now and the climate of the past, defined respectively by the GMST values of now and of the preindustrial past (1850-1900, based on the [Global Warming Index](#)), which differ by 1.2 °C. To statistically model the event under study, we use a generalised extreme value (GEV) distribution that shifts with GMST. Next, results from the ERA5 reanalysis and the individual CMIP6 models that pass the evaluation tests are synthesized into a single attribution statement.

There are some small differences between the model evaluation method used in this super-rapid analysis and a standard WWA analysis following the protocol. The model evaluation step here assesses the seasonal cycle and statistical fit parameters, but not the spatial pattern of the parameter field as in a standard WWA analysis.

3 Observational analysis: return period and trend

Using the ERA5- extended preliminary dataset, the magnitude of the event averaged over the box (land only) is 32.6 °C. Using a GEV that shifts with the smoothed GMST, we calculate the return period, change in intensity and probability ratio between 2023 and a past climate that is 1.2 °C cooler than now (i.e. without anthropogenic warming). Given the extremity of the event compared to the length of the time series, the return period has a large uncertainty, with a best estimate of about 400 years, and a lower estimate of 60 years (and an infinite upper bound). A final value for the return period may change for reanalysis data rather than preliminary data, but given the uncertainty around it we do not consider this to be a problem for the current rapid analysis. For the model analysis we use a return period of 400 years.

Due to the large trend and large return period the probability ratio is not well defined. Therefore we focus on the change in intensity, which is 3.5 °C (95% CI 1.7 °C to 5.3 °C).



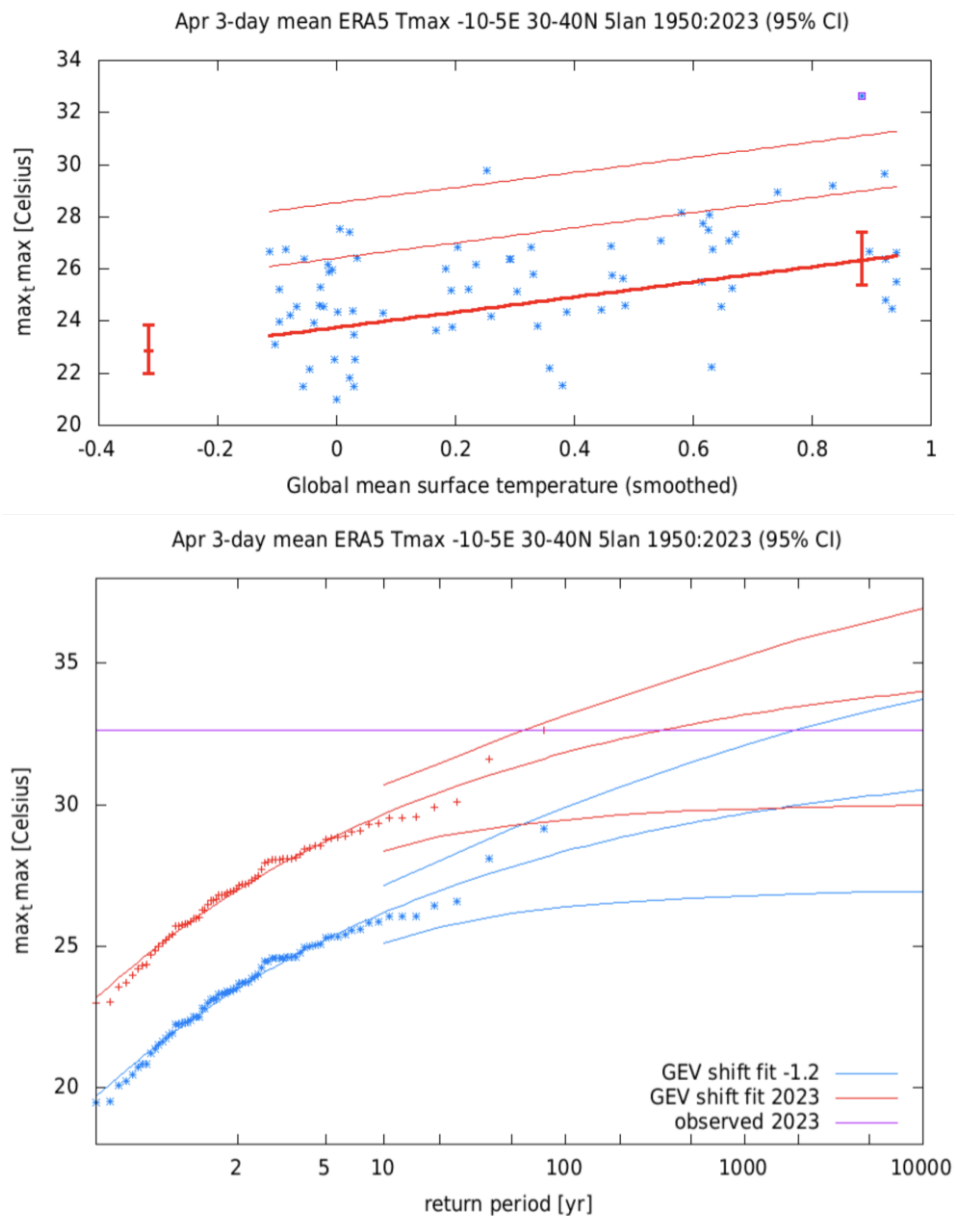


Figure 2. Top: Time series of AprTX3x along with the 10-year running mean (green line). Middle: AprTx3x over the study region estimated from ERA5 records to change in global mean temperature. The thick red line denotes the time-varying mean, and the thin red lines show 1 standard deviation (s.d) and 2 s.d above. The vertical red lines show the 95% confidence interval for the location parameter, for the current, 2023 climate and the hypothetical, 1.2°C cooler climate. The 2023 observation is highlighted with the magenta box. Bottom: Return periods for the 2023 climate (red lines) and the 1.2°C cooler climate (blue lines with 95% CI), based on ERA5 data.

4 Model evaluation

In this section we show the results of the model evaluation. We use all models that pass the evaluation tests with the label 'good' or 'reasonable', but not the ones with 'bad' or more than one reason to label with 'reasonable'. Table 1 shows the model evaluation results.

Table 1 Model evaluation values for the statistical parameters and seasonal cycle

Model / Observations	Seasonal cycle	Sigma	Shape parameter	Conclusion
ERA5		1.85 (1.50 ... 2.10)	-0.20 (-0.57 ... -0.10)	
ACCESS-CM2 historical-ssp585 (1)	good	2.25 (1.71 ... 2.54)	-0.19 (-0.44 ... -0.030)	reasonable, sigma small overlap
ACCESS-ESM1-5 historical-ssp585 (1)	good	1.79 (1.35 ... 2.06)	-0.20 (-0.37 ... -0.010)	good
CMCC-ESM2 historical-ssp585 (1)	good	1.98 (1.38 ... 2.34)	-0.17 (-0.39 ... 0.060)	bad, sigma too high
CNRM-CM6-1-HR historical-ssp585 (1)	good	2.16 (1.66 ... 2.50)	-0.16 (-0.33 ... 0.020)	reasonable
CNRM-CM6-1 historical-ssp585 (1)	good	2.09 (1.20 ... 2.48)	-0.11 (-0.26 ... 0.21)	good
CanESM5 historical-ssp585 (1)	reasonable	2.40 (1.85 ... -0.110)	-0.38 (-0.63 ... -0.16)	Reasonable 3x : sigma too high and reasonable seasonal cycle and high magnitude
EC-Earth3-Veg-LR historical-ssp585 (1)	good	2.10 (1.64 ... 2.37)	-0.26 (-0.59 ... -0.020)	reasonable
EC-Earth3-Veg historical-ssp585 (1)	good	2.18 (1.78 ... 2.50)	-0.59 (-0.44 ... 0.030)	reasonable
EC-Earth3 historical-ssp585 (1)	good	2.79 (2.09 ... 3.26)	-0.40 (-0.63 ... -0.15)	bad, sigma too high
INM-CM4-8 historical-ssp585 (1)	good	1.97 (1.32 ... 2.33)	-0.29 (-0.54 ... -0.080)	graph looks bad
INM-CM5-0 historical-ssp585 (1)	good	2.44 (1.84 ... 2.82)	-0.20 (-0.47 ... -0.040)	Reasonable 2x, statistics and high magnitude
IPSL-CM6A-LR historical-ssp585 (1)	good	2.33 (1.53 ... 2.78)	-0.14 (-0.31 ... 0.11)	reasonable
MIROC6 historical-ssp585 (1)	reasonable, but way too steep	2.12 (1.61 ... 2.46)	-0.22 (-0.38 ... -0.040)	bad, 2x reasonable and very high magnitude
MPI-ESM1-2-HR historical-ssp585 (1)	good	1.88 (1.39 ... 2.16)	-0.28 (-0.48 ... 0.030)	reasonable
MPI-ESM1-2-LR historical-ssp585 (1)	good	1.70 (1.30 ... 2.01)	-0.050 (-0.28 ... 0.13)	good
MRI-ESM2-0 historical-ssp585 (1)	good	2.41 (1.82 ... 2.70)	-0.28 (-0.58 ... -0.020)	bad, sigma too high
NorESM2-LM historical-ssp585 (1)	good	1.67 (1.10 ... 1.95)	-0.24 (-0.51 ... 0.010)	bad. big jump in temperature in 1950
NorESM2-MM historical-ssp585 (1)	good	1.54 (1.08 ... 1.82)	-0.18 (-0.43 ... 0.010)	reasonable
TaiESM1 historical-ssp585 (1)	good	2.18 (1.55 ... 2.53)	-0.26 (-0.42 ... -0.080)	reasonable

5 Multi-method multi-model attribution

This section shows Probability Ratios and change in intensity ΔI for models that passed the evaluation tests and also includes the values calculated from the fit with observations.

Table 2: Probability Ratio and change in intensity in AprTx3x for the models that passed the validation tests.

		Past-present (-1.2°C)		Present-future (+0.8°C)	
Model / Observations	Threshold for return period 400 yr	Probability ratio PR [-]	Change in intensity ΔI [°C]	Probability ratio PR [-]	Change in intensity ΔI [°C]
ERA5	32.6 °C	1.0e+4 (15 ... 1.0e+4)	3.5 (1.7 ... 5.3)		
ACCESS-CM2 historical-ssp585 (1)	32.3 °C	1.9e+2 (1.3 ... ∞)	1.3 (-0.12 ... 2.6)	0.14 (0.0020 ... ∞)	-1.1 (-1.5 ... -0.74)
ACCESS-ESM1-5 historical-ssp585 (1)	34.2 °C	1.5e+3 (6.4 ... ∞)	2.2 (1.2 ... 3.3)	0.11 (0.0040 ... ∞)	-1.6 (-2.0 ... -1.2)
CNRM-CM6-1-HR historical-ssp585 (1)	32.2 °C	1.1e+2 (2.9 ... ∞)	1.9 (0.57 ... 3.1)	0.31 (0.0070 ... ∞)	-0.86 (-1.3 ... -0.51)
CNRM-CM6-1 historical-ssp585 (1)	34.3 °C	8.6 (2.1 ... ∞)	1.8 (0.86 ... 2.9)	0.34 (0.0040 ... ∞)	-0.91 (-1.4 ... -0.44)
EC-Earth3-Veg-LR historical-ssp585 (1)	32.2 °C	∞ (1.4 ... ∞)	1.2 (-0.12 ... 2.4)	0.21 (0.0060 ... ∞)	-0.87 (-1.4 ... -0.32)
EC-Earth3-Veg historical-ssp585 (1)	34.1 °C	36 (1.9 ... ∞)	1.4 (0.24 ... 2.5)	0.21 (0.0060 ... ∞)	-1.0 (-1.4 ... -0.57)
IPSL-CM6A-LR historical-ssp585 (1)	31.1 °C	2.1e+3 (3.4 ... ∞)	1.6 (0.43 ... 2.9)	0.13 (0.0070 ... ∞)	-1.2 (-1.6 ... -0.66)
MPI-ESM1-2-HR historical-ssp585 (1)	32.6 °C	∞ (25 ... ∞)	2.3 (1.1 ... 3.5)	0.096 (0.0020 ... ∞)	-1.3 (-1.8 ... -0.83)
MPI-ESM1-2-LR historical-ssp585 (1)	32.0 °C	5.9e+2 (4.5 ... ∞)	1.9 (0.66 ... 3.1)	0.085 (0.0040 ... ∞)	-1.5 (-2.0 ... -1.0)
NorESM2-MM historical-ssp585 (1)	32.4 °C	∞ (2.2 ... ∞)	1.4 (0.070 ... 2.9)	0.16 (0.0040 ... ∞)	-0.88 (-1.3 ... -0.35)
TaiESM1 historical-ssp585 (1)	34.4 °C	∞ (8.4 ... ∞)	1.6 (0.19 ... 2.9)	0.12 (0.0030 ... ∞)	-1.0 (-1.4 ... -0.72)

6 Hazard synthesis

For the event definitions described above we evaluate the influence of anthropogenic climate change on the events by calculating the probability ratio as well as the change in intensity using observations and climate models. Models which do not pass the evaluation tests described above are excluded from the analysis. The aim is to synthesise results from models that pass the evaluation along with the ERA5 reanalysis, to give an overarching attribution statement. Figure 3 shows the changes in intensity for the observations (blue) and models (red) for the past and future. The dark red bar shows the model average, consisting of a weighted mean using the (uncorrelated) uncertainties due to natural variability. Observation-based products and models are combined into a single result in two ways. Firstly, we neglect common model uncertainties beyond the intermodel spread that is depicted by the model average, and compute the weighted average of models (dark red bar) and observations (dark blue bar): this is indicated by the magenta bar. As, due to common model uncertainties, model uncertainty is larger than the intermodel spread, secondly, we also show the more conservative estimate of an unweighted, direct average of observations (dark red bar) and models (dark blue bar) contributing 50% each, indicated by the white box around the magenta bar in the synthesis figures.

The probability ratio is too high to properly synthesise; a synthesis, in which all infinities have been changed into 10000, results in a lower bound of about 100, and best estimates are much higher. The high numbers lead us to the qualitative conclusion that temperatures as high as observed would have been extremely unlikely to occur if human activities had not warmed the climate by 1.2 °C. We only report quantitative changes in the heat intensity. The intensity change in reanalysis data ranges from 1.7 °C to 5.3 °C. All models that passed the evaluation tests show a similar trend, but the trend in the models is much lower than in ERA5. The model average ranges between 1.4 °C and 2.1 °C. Therefore we use the unweighted, direct average of observations and the model average. This gives us a conservative estimate of the change intensity of about 2°C with uncertainty ranging from 1.7 °C to 3.5 °C. For the future, 0.8 °C warmer climate, the model best estimate of a change in intensity is about another 1°C with uncertainty ranging from 0.8 °C to 1.5 °C.

Combining lines of evidence from the synthesis results of the past climate, results from future projections and physical knowledge we focus on communicating the best estimate and uncertainty of the intensity change for the past and future climate as well as the qualitative statement that an event like this would have been almost impossible to occur without human-induced climate change.

Note that as in previous studies of heat waves in neighbouring Western Europe (e.g., [WWA 2022](#), [Van Oldenborgh et al., 2019](#)), models tend to underestimate the intensity change relative to reanalyses, a fact that is not yet well understood.

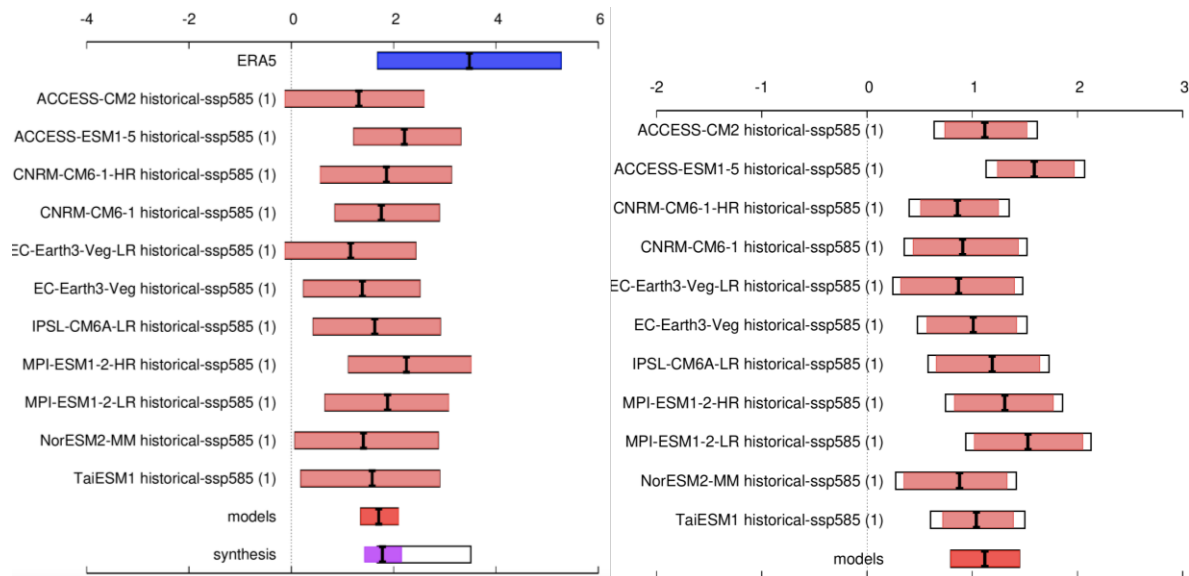


Figure 3. Synthesis of intensity change when comparing the 400-yr event to a 1.2 °C cooler climate (left) and comparing to a 0.8 °C warmer climate (right).

7 Vulnerability and exposure

Heatwaves are amongst the deadliest natural hazards with thousands of people dying from heat-related causes each year ([EM-DAT](#)). However, the full impact of a heatwave is often not known until weeks or months afterwards, once death certificates are collected, or scientists can analyse excess deaths. While verified data from the current heatwave are not yet available, we do know that in 2022 heatwaves contributed to nearly 4000 deaths in Spain and over 1000 deaths in Portugal ([WHO, 2022](#)). Every year, an average of 262, 250, and 116 people die from heat-related illness in Algeria, Morocco, and Tunisia, respectively ([Hajat et al., 2023](#)). In Tunis, a review of all-cause mortality between 2005-2007 found that for every degree Celcius over 31.5C, the daily mortality increased by 2% ([Bettaieb et al., 2020](#)). Early season heatwaves tend to be particularly deadly because of a lack of acclimatisation of the population, lower preparedness for heat (e.g. people have not yet brought out fans or A/Cs from storage), and harvesting effects ([Gasparrini et al., 2016](#); [Lee et al., 2014](#)).

For example, a mild winter such as the one experienced across Europe in 2022-23 ([Reuters, 2023](#)) is known to influence the composition of at-risk groups by sustaining a greater pool of vulnerable people to later in the year, heightening the mortality risk in warmer months, particularly to early bouts of heat ([Åström, Forsberg and Rocklöv, 2011](#)). Preceding winter mortality linked to influenza as well as respiratory and cardiovascular disease further modify the mortality risk for summer time ([Rocklöv, Forsberg and Meister, 2008](#)), explaining why the COVID-19 pandemic is noteworthy. In addition, urban areas tend to be hotter due to the urban heat island effect, and one study in Spain found that vulnerability in urban areas was six times higher than in rural areas, with factors like working conditions, and the number of people living homes in poor conditions driving vulnerability ([Lopez-Bueno et al., 2022](#)).

The link between extremely high temperatures and an increase in mortality is well established, globally as well as across the countries studied for this type of event ([Rodrigues, Santana and Rocha, 2021](#); [Royé et al., 2020](#); [Ahmadalipour and Moradkhani, 2018](#); [Green et al., 2019](#)). However, heatwaves do not need to result in excess deaths, especially in dry heat cases. Heat interventions can be as simple as

checking on your neighbours, drinking enough water, and avoiding exposure to heat and direct sun during the hottest hours of the day and can go a long way in saving lives ([Singh et al., 2019](#)). Further, key to fostering resilience is governments' systematic implementation of measures to help communities and vulnerable groups cope with the shock, including ensuring widespread access to cooling devices and that the energy grid can withstand the increased power demand, as well as preparing health services for an influx of patients suffering heat-related illnesses ([Casanueva et al., 2019](#)). Notably, research shows that heat-related fatalities have indeed decreased following the Spanish government's implementation of the national Heat Health Prevention Plan in 2004, the need for which was highlighted by the devastating 2003 European heatwave ([Martínez-Solanas and Basagana, 2019](#)). Buildings that minimise the effect of heat (design and material) with urban planning for extreme heat moreover tend to be cooler, in part by reducing the urban heat island effect through incorporating more green and blue spaces which has proved effective in e.g. Lisbon, Portugal ([Burkart et al., 2016](#)). In Morocco, a National Multi-Risk Plan for Public Health Emergency Preparedness and Response is in development and will include early warning and early action for heatwaves which have been identified as a key risk to public health ([MoH Morocco](#)).

This outstanding early heat episode comes at the time of growing for many crops such as wheat, and on top of a multi-year drought in the exposed regions with pre-existing water resource deficit. This situation was judged “alarming” in Morocco ([Atalayar, 2023](#)) as it could jeopardise the whole agricultural season, with a fall already of 80% of irrigation water ([Morocco World News, 2023](#)). This highlights the cascading impacts that heatwaves, in combination with other hazards, can have on the economy, livelihoods, and health ([Zachariah et al., 2022](#)).

The results of the study, showing a larger increase in intensity of heat in the observations than climate models, indicate the need to work urgently to put into place adaptation interventions that are known to reduce heat-related mortality and its knock-on effects.

Data availability

All data will become available via the [KNMI Climate Explorer](https://climexp.knmi.nl): <https://climexp.knmi.nl>

References

All references are given as hyperlinks in the text.

Please cite this paper as:

Philip, S; Kew, S; Vautard, R; Pinto, I; Vahlberg, M; Singh, R; Driouech, F; Lguensat, R; Barnes, C; Otto, FEL (2023). Extreme April heat in Spain, Portugal, Morocco & Algeria almost impossible without climate change.

DOI: <https://doi.org/10.25561/103833>.

This work is licensed under a Creative Commons Attribution-NonCommercial-No-Derivatives 4.0 International License.



DOI: <https://doi.org/10.25561/103833>.